JEE Journal of Ecological Engineering

Journal of Ecological Engineering 2024, 25(11), 109–123
https://doi.org/10.12911/22998993/192671
ISSN 2299–8993, License CC-BY 4.0

Received: 2024.08.02
Accepted: 2024.09.23
Published: 2024.10.01

Treatment of Wastewater from Oil Refineries by a Combination of Electrocoagulation with Photocatalytic Processes Using Immobilized Nano-Zinc Oxide Photocatalyst

Qasem Kadhum Hameed[1*], Wadood Taher Mohammed[1]

[1] Chemical Engineering Department, College of Engineering, University of Baghdad, Baghdad, Iraq

* Corresponding author's e-mail: qasem.kadhum2107m@coeng.uobaghdad.edu.iq

ABSTRACT

The present work aimed to reduce the COD of petroleum refinery wastewater using individual and combined processes based on the electrocoagulation and photocatalytic process with immobilized nano-zinc oxide. Also, energy savings alongside performance improvements were evaluated within this conglomerated system. Results showed that the removal efficiency of COD was 72% after 120 min when using electrocoagulation process under the given conditions (15 mA/cm^2, pH of 7, and flow rate of 0.5 L/min). Regarding the process involving photocatalysis, the removal efficiency of COD was 76% after 120 min under the analyzed conditions (ZnO concentration of 80 g/m^2, pH of 7, power of irradiation equal to 65 W, and flow rate of 0.5 L/min). Several combined sequential and simultaneous systems were tested. Results confirmed that the simultaneous photo-EC system operated at 30 min is the best one and has the ability to achieve COD removal of 82% under the studied conditions (15 mA/cm^2, pH of 7, and flow rate of 0.5 L/min, ZnO concentration of 80 g/m^2, and 65 W). Furthermore, the further notable features of the combined simultaneous photo-EC system were operating at shorter operation time and lowering dissolution rate of anode electrode (0.2 gram) that makes the system to be the most economic process with an energy consumption of 28.44 kWh/kg COD.

Keywords: electrocoagulation, nano- bio-zinc oxide, photocatalytic, immobilizing, wastewater.

INTRODUCTION

The industrial sector is witnessing advancements and progress owing to various manufacturing techniques being implemented (Zhang et al., 2015; Elmobarak et al., 2021). Consequently, industrial areas are continually generating large volumes of wastewater at rapid rates, often discarding it without proper handling and treatment measures in place. Petroleum refineries and related industries play a pivotal role in economic growth (Varjani et al., 2019; Jafarinejad, Jiang, 2019). Refineries are met with the significant task of handling wastewater disposal. The wastewater that originates from the industries based on petroleum industry contains a variety of organic and inorganic contaminants. These contaminants include, but are not limited to, sulfides, phenol, BTEX (Benzene, Toluene, Ethylbenzene, Xylen), hydrocarbons, and heavy metals (Abdulredha et al., 2020; Raza et al., 2019). Research indicates that within the next 20 years, the worldwide demand for oil is projected to surge to an estimated 107 million barrels each day. By the year 2030, oil is expected to account for approximately 32% of the planet's energy consumption (Keramati, Ayati, 2019). Concurrently, the practice of discharging wastewater by oil producing companies and refineries into natural environments is escalating, posing a significant risk to the world's water reserves (El-Naas et al., 2014).

The petroleum industry is responsible for generating large volumes of dangerous substances. This occurs through various stages, such as the extraction of oil, refining, transporting, and storing, all of which pose significant risks to both environmental and human health (Varjani 2017; Jiménez et al., 2019). Many techniques have been used to treat oil refinery wastewater, such as chemical precipitation, adsorption, wet oxidation,

vacuum catalytic distillation, coagulation and flocculation, photocatalytic oxidation, Fenton process, and ozone (Almomani et al., 2016; Al Mayyahi, Al-Asadi, 2018). Physical strategies, although extensive in time, simply relocate the contaminants to a different phase. Biological approaches fall short in effectiveness as they fail to break down oil hydrocarbons, which are stubborn against biodegradation processes. In contrast, the use of electrochemical techniques has gained popularity in recent times due to their advantages (Al Mayyahi, Al-Asadi, 2018).

Electrochemical techniques have become increasingly popular for their wide range of benefits. Known as electrocoagulation (EC), this method applies electrochemistry principles for wastewater treatment (Wan et al., 2023). An electric current is introduced into the water, causing pollutants to become unstable. Through this process, coagulants (like iron and aluminum hydroxides) are produced, which neutralize pollutant charges and aid in their extraction (García-García et al., 2015). For example, applying an electrical current to a cell with a stainless-steel cathode and an aluminum anode result in aluminum ions being produced from the anode surface. These aluminum ions react with the OH^- ions generated at the cathode through water reduction, forming amorphous aluminum hydroxide ($Al(OH)_3(s)$) flocs (Equations 1–4). Concurrently, oxygen and hydrogen gases are released at the anode and cathode, respectively (Equations 2, 3). These gases help in the flotation of flocs to the surface of the liquid, while the heavier flocs settle at the bottom of the cell through sedimentation (García-García et al., 2015). The electrocoagulation process involves the following reaction:

- at the anode:

$$(Al)_{(s)} \rightarrow Al_{(a)}{}^{+3} + 3e^- \quad (1)$$

$$2H_2O \rightarrow O_{2(a)} + 5H^+ + 5e^- \quad (2)$$

- at the cathode:

$$2H_2O + 2e^- \rightarrow H_2 + 2OH^- \quad (3)$$

- in the bulk:

$$Al^{+3} + 3OH^- \rightarrow Al(OH)_{3(s)} \quad (4)$$

Advanced oxidation process (AOP) is a technique for the formation of hydroxyl radicals used for oxidation the organic pollutants in wastewater (Cao et al. 2020; Sathasivam et al., 2019).The hydroxyl radical is known for its strong ability to oxidize (E_0 = 2.8 V), making it capable of reacting with virtually all kinds of organic materials (Yang, Hoffmann 2016; Li et al., 2018). This leads to their complete breakdown into carbon dioxide (CO_2), water, and inorganic salts, or transforms them into less harmful compounds (Qu et al., 2018; Rostam, Taghizadeh, 2020). Advanced oxidation processes (AOPs) offer significant benefits, including the elimination of pollutants and prevention of harmful compound generation, which surpass the efficacy of conventional water treatment methods (Ghanbari et al., 2020; Sonu et al., 2019). Photoctalytic process is one of AOPs that are used in treatment of wastewater efficiently. The mechanism of photocatalytic oxidation involves a series of processes. This occurs when the energy hitting the surface meets or exceeds the energy gap, leading to the creation of electron-hole pairs in semiconductor particles. Subsequently, electrons move from the valence band to the conduction band, resulting in the formation of holes in the valence band. These holes possess a high capacity for oxidation, whereas the excited electrons are highly capable of reduction. The reactive hole is then oxidized, generating hydroxyl radicals as it reaches the surface and gives up its electron. Conversely, electrons are utilized in the reduction process. As a result, semiconductor particles serve dual functions as receivers and donors of electrons for molecules in their surroundings (Adnan et al., 2020). Equations (5–11) represent the mechanism of photocatalytic oxidation (photo/metal oxide (MO)):

- starting reaction:

$$MO + h\nu \rightarrow MO\ (h^+ + e^-) \quad (5)$$

- oxidative reactions

$$h^+ + H_2O \rightarrow H^+ + \bullet OH \quad (6)$$

$$2h^+ + 2\,H_2O \rightarrow 2H^+ + H_2O_2 \quad (7)$$

$$H_2O_2 \rightarrow 2\,\bullet OH \quad (8)$$

- reductive reactions

$$e^- + O_2 \rightarrow \bullet O_2^- \quad (9)$$

$$O_2^- + H_2O + H^+ \rightarrow H_2O_2 + O_2 \quad (10)$$

$$H_2O_2 \rightarrow 2\,\bullet OH \quad (11)$$

The combination of EC with photocatalytic oxidation results in obtaining high removal efficiency with lower energy consumption due to the synergistic effects of the two processes. Therefore, the aim of present work was to apply the two process sequentially or simultaneously for treating petroleum refinery wastewater and to explore which the combination system give better removal with lower energy consumption.

MATERIAL AND METHODS

Most of previous works regarding EC and photocatalytic process used batch-type mode for reactors. While in the present study, batch recycling mode was used for reactors operated as combined system. Nanoparticle zinc oxide was used as a photocatalyst. It was supplied by Sigma-Aldrich Company having the following characteristics: 30 nm particle size, 48 m^2/g surface area, and 0.0581 cm^3/g pore volume. Concrete was chosen for the photoreactor floor and to immobilize nanoparticles due to its practical application and cost-efficiency.

Wastewater characterization

In this study, the wastewater from Al- Diwaniyah oil refinery in Iraq served as a sample for research and investigation. This sample was characterized by containing heavy and light hydrocarbon compounds, Table 1 presented its qualities.

Electrocoagulation reactor

A cylindrical electrocoagulation reactor (semi-batch) was constructed from Plexiglas, as it can be seen in Figure 1. It was composed of three cylindrical sections, each with varying sizes. The upper segment measures 70 cm in outer diameter, 55 cm in length, and 4 cm in thickness. The central section measures 70 cm in outer diameter, 70 cm in length, and 4 cm in thickness, the dimensions of the bottom section are identical to those of the upper section. Two electrodes were utilized, one made of the AU4G aluminum alloy (anode) featuring a cylindrical shape with an outside diameter of 60 mm, a length of 55 mm, a thickness of 5 mm, and an effective surface area of 78.5 cm^2. The other electrode (cathode) was made of stainless steel, shaped as a rod with an outer diameter of 28 mm and a length of 107 mm. These were operated at a water flow rate of 0.5 liters per minute. The spacing between the electrodes was set to 11 millimeters. The cathode electrode, which extended 52 mm before the point where it enters at the top and reaches the center of the anode, was designed longer than the anode to facilitate the escape of hydrogen gas generated at the cathode. This arrangement is critical for enabling the flotation of suspended solids outside the reactor.

Photocatalytic reactor

The photocatalytic reactor was designed as a water conduit, depicted in Figure 2. The

Table 1. Qualities of effluents from the Diwaniyah oil refinery

Parameter	pH	COD (mg/l)	Turbidity (NTU)	Conductivity (mS/cm)	Phenol (mg/l)	T.D.S. (mg/l)	SO_4^{-2} (mg/l)	Cl^- (mg/l)
Value	7	1278	25.6	11.5	13.6	4575	122	2055

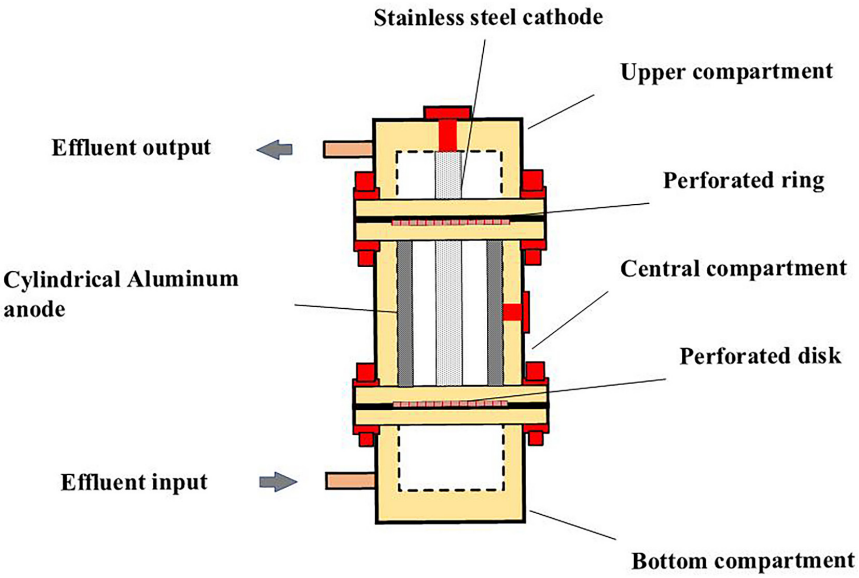

Figure 1. Schematic diagram of the electrocoagulation reactor

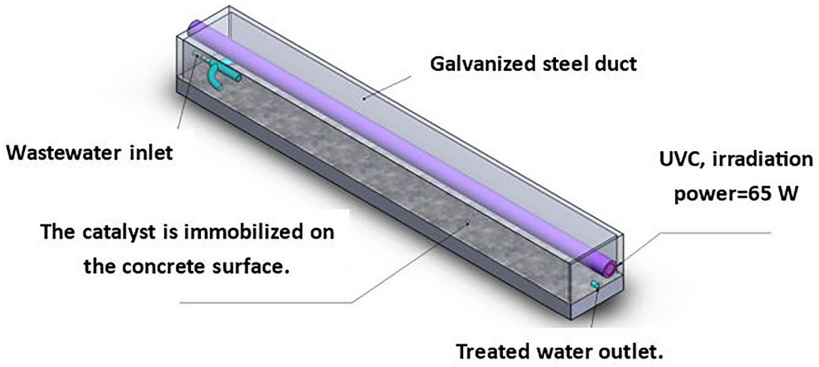

Figure 2. Schematic diagram of photoreactor

photoreactor is constructed from Calvinize, a material known for its resistance to corrosion, and measures 90 by 11 by 10 centimeters. The entire surface of the reactor was illuminated by a 65-watt UVC lamp, measuring 90 cm in length, positioned 5 cm above the wastewater surface. The rate at which fluid (wastewater) enters the reactor was maintained at 0.5 liter per minute and the layer of contaminated water in motion measures 3 mm in thickness, while the dimensions of the concrete layer measured 900 cm^2 in surface area and 3 cm in thickness. Previous studies have led to the selection of a specific concrete blend designed to support the adherence of nano-zinc oxide particles on its surface (Delnavaz et al., 2011). Table 2 presents a detailed overview of the hydraulic and volumetric properties of the reactor.

Experimental set-up

Figure 3 shows the integrated batch-recycle setup being analyzed. This system comprises an electrochemical reactor and a photoreactor, linked to a 1.5 – liter reservoir tank. It also includes a pulse pump (type- HYBL5LNPVF001, Italy) and a recycling pump, each with a capacity to circulate 500 ml per minute, aimed at moving and recycling contaminants. These pumps are connected to a tank that circulates the solution to maintain uniformity of the waste, ensure the release of hydrogen gases, and prevent foaming, which could reduce the effectiveness of electrocoagulation. Additionally, an air pump (model-ACO-208, 45 W China) was attached to the circulation tank for saturating the solution with oxygen for the completion of the photocatalysis process. Also included are a liquid flow meter (type-ZY-IA, 25–1000 ml/min), an air flow meter (0–500 ml/min), and various valves intended for different functions. An electronic pH meter was employed to ascertain the pH levels of the electrolyte (type - PH211, HNNA Instrument Inc. Romania).

Table 2. The hydraulic and volumetric properties of the reactor

Parameters	Value
Reactor's effective capacity	270 cm^3
Effluent velocity	2.78 cm/s
Effluent rate	500 cm^3/min
Thickness of the flow layer	3 mm
reactor slope	0.3
Distance of the UV Lamp	5 cm

Operational tasks involve connecting both the electrodes and the photoreactor to a digital DC power supply (UNI-T, UTP3315TFL-II, China). To sustain the system's efficiency, the electrodes, and the floor of the photoreactor were meticulously cleaned. All experiments were performed at a temperature of 25 °C.

Following the assessment of acidity with 1 M HCl or 1 M NaOH, 1.25 liters of wastewater was transferred to the reservoir. The appropriate electrical current was then selected. At fixed intervals, samples were taken for analysis. The samples were filtered using filter paper to eliminate any suspended particles and left to settle for 24 hours. To determine the chemical oxygen demand (COD), measurements were taken every 15 minutes throughout the treatment using a thermos-reactor (Model: RD-125) and a spectrophotometer (Model: MD-200), both provided by Lovibond. Each run included three COD measurements, and the average was used for this study.

In this study, series of tests were performed to treat wastewater from oil refineries using various techniques and systems based on a recirculating batch process. A brief description of these

is provided below: First: Individual systems, wastewater treatment involved the use of two individual processes: electrocoagulation and photocatalysis in separate stages for 120 minutes for each process. Second: Sequential EC-photo system-1: in this setup, contaminants are first treated in an electrocoagulation reactor for 60 minutes. After that, it undergoes an additional 60 – minute treatment process individually in the photoreactor. Third: Sequential Photo-EC system -1: In this setup, contaminants first go through a 60 – minute treatment in the photoreactor followed by a similar duration of treatment in the electrocoagulation reactor, with each treatment conducted individual (two stages). Fourth: sequential EC-photo system-2 and sequential Photo-EC system-2: These systems resemble the second and third ones, with the primary distinction being that each treatment process lasts 30 minutes instead of 60 minutes(two stages). Fifth: Simultaneous EC-photo system: Contaminants first move through the electrochemical reactor and subsequently travel in series to the photoelectric reactor with a duration of 120 minutes (The system functions with a single simultaneous stage.). Sixth: Simultaneous Photo-EC system: contaminants first move into the photoelectric reactor and subsequently flow through the electrochemical reactor one after the other lasting 120 minutes (The system functions with a single simultaneous stage).

Calculations and analytical methods

The effectiveness of COD removal was evaluated using Equation 12 (Demirbas, Kobya, 2017):

$$RE\% = \frac{CODo\_COD}{CODo} \times 100 \quad (12)$$

where: $RE\%$ indicates the effectiveness of removal. Here, COD_o – represents the initial measurement of chemical oxygen demand, expressed in mg/L; whereas COD refers to the subsequent measurement of chemical oxygen demand, also measured in mg/L.

The energy consumption, expressed as kilowatt-hours per kilogram of COD removed, was calculated using Equation 13 (Yavuz, Ögütveren, 2018; Fahem, Abbar, 2020):

$$SEC = \frac{U \cdot I \cdot t}{(COD_o - COD)V} \quad (13)$$

where: SEC is defined as a specific energy consumption. U is the term used for electrical potential, measured in volts (V). I represents the intensity of the current in amperes (A), while t is used to denote the duration of the reaction in hours (hr.), and V is the volume of wastewater measured in liters (L). Additionally, the terms COD_o and COD represent the chemical oxygen demand concentrations at the beginning

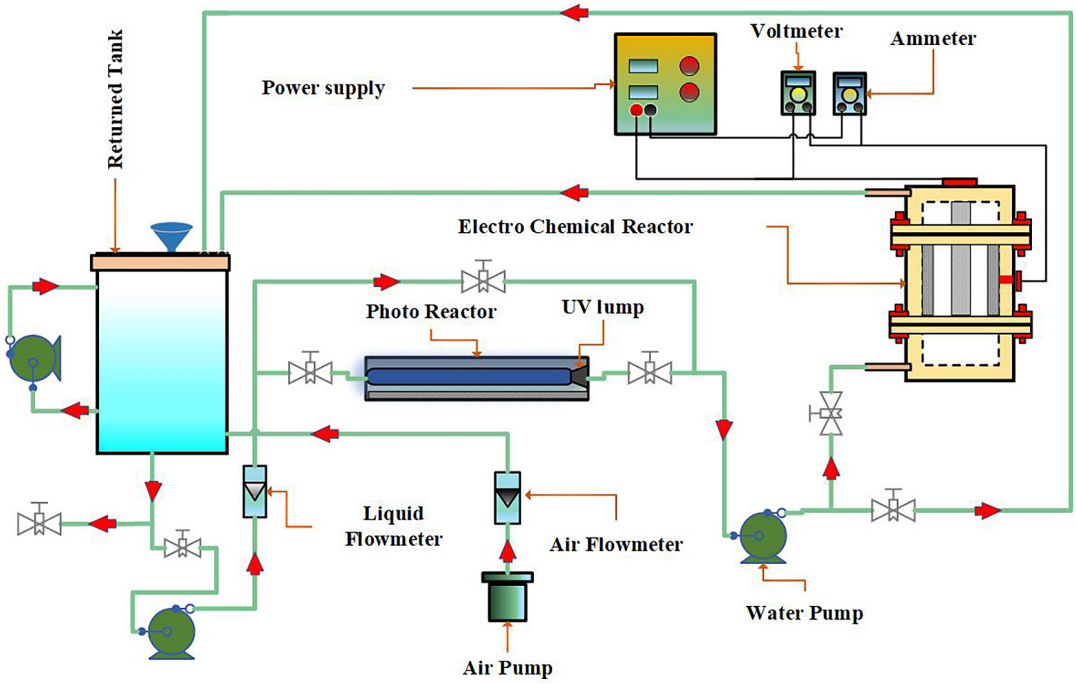

Figure 3. Schematic diagram of experimental set-up

and at time *t*, respectively, quantified in grams per liter (g/L).

The degradation rate and the dissolution of the anode are impacted by the electric current flowing through the impure liquid and the length of the reaction time, denoted as (*t*). The determination was made using the application of Faraday's law, as demonstrated in the Equation 14 (Demirbas, Kobya, 2017):

$$m = \frac{I \cdot t \cdot M}{F \cdot z} \quad (14)$$

where: the symbol (*m*) signifies the mass of the metal that has dissolved, measured in grams, while (*t*) indicates the time span of the electrolysis in seconds. Additionally, (*M*) is the molecular mass of aluminum, specifically 26.98 g/mol, and (*F*) represents Faraday's constant, which is equal to 96485 C/mol. Furthermore, (*z*) is used to show the valence of the metal, which is 3 for aluminum.

RESULTS AND DISCUSSION

Individual systems

Figure 4 represents the removal of COD by the individual processes, namely electrocoagulation and photocatalytic processes. EC was operated at 15 mA/cm^2, pH = 7 with a flow rate of 0.5 L/min. while photocatalytic process was operated at catalyst dosage of 80 g/m^2,an air flow rate of 100 ml/min, wastewater flow rate of 0.5 L/min, UVC lump of 65W and pH = 7. Figure 4 indicates that after a period of 120 minutes, the treatment efficiency achieved by an electrocoagulation process was 72%, and by photocatalytic process was 76%. The figure clearly indicates that, within the initial 15 minutes duration, electrocoagulation has 8% higher purification efficiency compared to photocatalysis. However, on-going time to reach 30 minutes, photocatalysis starts to surpass electrocoagulation in terms of effectiveness. This shift in efficiency can be attributed to an increase in the production of hydrogen, which in turn weakens the ability of the electrocoagulation process to absorb pollutants.

Additionally, repeated experiments with the photocatalytic process revealed a gradual decline in its performance. This reduction stems from the gradual removing of the catalyst immobilizing on the concrete surface, due to continual contact with polluted substances (Keramati, Ayati, 2019).

Combined systems

Sequential EC-photo system-1 and sequential photo -EC system-1

Figure 5 shows a comparison between sequential EC-photo system-1 and sequential photo-to-EC system-1 in which EC and photocatalytic processes were operated under the same conditions in section 3.1 except the time here was 60 min for each process.

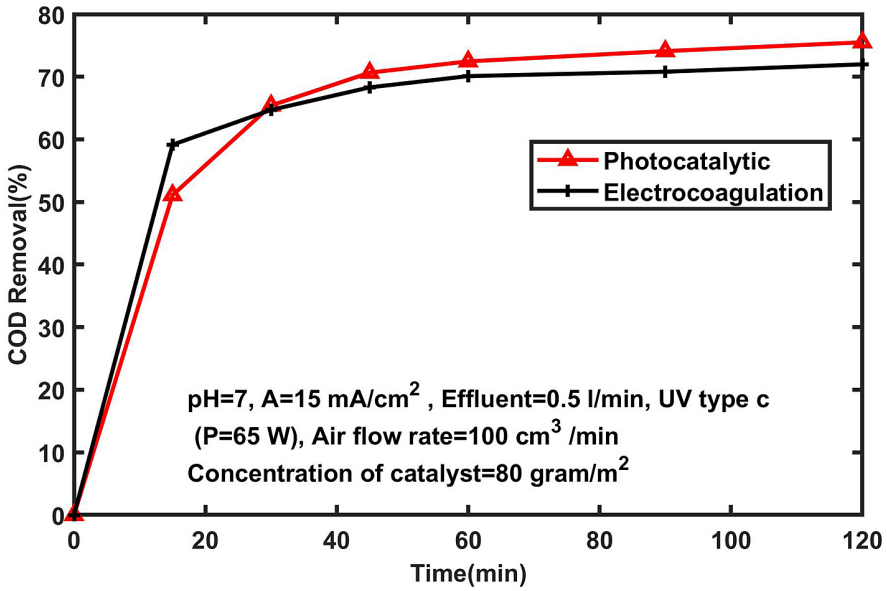

Figure 4. COD removal at photocatalytic and electrocoagulation processes

Figure 5 shows that sequential EC-photo system-1and sequential photo-EC system-1 have contamination removal efficiencies of approximately 71% and 82%, respectively. The data also shows that after 60 minutes, sequential EC-photo system-1efficiency levels out at around 70% and does not change through the rest of the two-hour treatment period. This level is due to the initial formation of a slurry during the first stage of the electrocoagulation process, which starts in the first hour. Adding a photocatalytic process in the second stage after the first hour does not significantly affect the efficiency of the sequential EC-photo system-1. Conversely, sequential photo -EC system-1 begins with the photocatalytic process at the first stage, avoiding slurry production and thus maintaining high efficiency from the start. In the second hour, the effluent from photo system transitions to the electrocoagulation process in the second stage, which further enhances its ability to remove contaminants seamlessly, outperforming combined sequential EC-photo system-1 in terms of removal rate.

Numerous researchers in water treatment have employed a two-stage sequential approach. Initially, they applied electrocoagulation in an alkaline environment. Following this, they removed the sludge and adjusted the pH to an acidic level, preparing the system for the second stage, which involved photocatalytic treatment. Consequently, their research demonstrated high effectiveness in treating simulated wastewater over extended periods and yielded results comparable to those presented in this paper when addressing actual wastewater conditions.

Mahdieh and Ayati explored the treatment of wastewater produced by oil refineries using a separate system in a simulated environment. They achieved a high removal efficiency of about 97% after 180 minutes of operation (Keramati, Ayati, 2019). In another research, scientists applied a two-stage process involving electrocoagulation and subsequent photocatalysis with titanium oxide to treat oily wastewater. Their method achieved COD reduction of approximately 72% (Al-Rubaiey, Albrazanjy, Kadhim, 2022).

In contrast, the conducted research yielded a removal efficiency of around 82% with sequential system (photo -EC system-1) and a novel approach but required only 120 minutes of operation.

Effect of parameters in the sequential Photo-EC system-1

Effect of current density

The rate of the reactions within the EC depends heavily on the electric current density, while photocatalytic activity is not affected by variations in current density. in EC, electrical flow primarily governs the generation of aluminum ions at the anode, determines the concentration of coagulants present, and influences the size of hydrogen bubbles produced at the cathode. As illustrated in Figure 6, after a set treatment time of 120 minutes, the removal efficiencies for

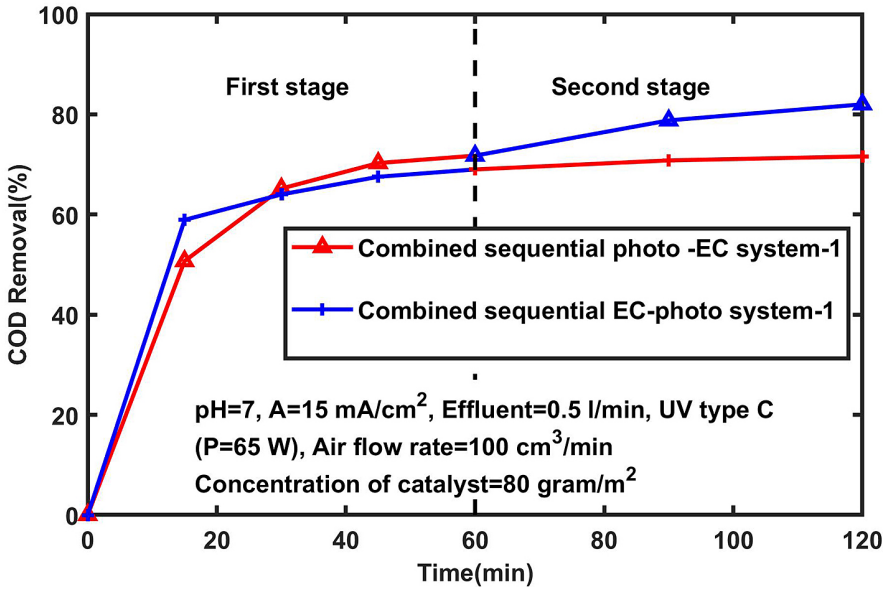

Figure 5. Combined sequential EC-photo system-1 + combined sequential photo -EC system-1

pollutants were recorded at 68%, 74%, 82%, and 78% corresponding to current densities of 5, 10, 15, and 20 mA/cm^2, respectively. As demonstrated in Figure 6, increasing the electric current from 5 to 15 mA/cm^2 enhances the efficiency with which pollutants are removed. However, when the current reaches 20 mA/cm^2, the removal efficiency diminishes to 78%.

This reduction in COD with increasing current density from 5 to 15 mA/cm^2 can be attributed to the influence of electric current on the generation rate of metal ions at the anode electrode as well as the formation rate and size of hydrogen bubbles generated at cathode electrode. These factors in turn affect the efficiency of the electrochemical coagulation reactions (Hariz et al., 2013). Further increasing the electric current leads to more rapid corrosion of the anode and a greater amount of coagulation.

As indicated in Figure 6, raising the current density beyond 15 mA/cm^2 resulted in diminished pollutant removal efficiency. This reduction is attributed to an increase in coagulation amount, complicating the oxidation processes (Kazeminezhad, Sadollahkhani 2016). Consequently, employing high current densities proves ineffective for maximizing removal efficiency. Ultimately, a current density of 15 mA/cm^2 was selected as the best for achieving 82% efficiency in removing pollutants. Many researchers have examined the influence of current on the removal rate in EC, revealing that increasing the current past a certain threshold negatively impacts the removal rate (Demirbas, Kobya 2017). Their findings align with the results obtained in the present research.

Effect of initial pH

In the photocatalytic process, the pH level influences not only the generation of hydroxide radicals but also impacts the surface characteristics of the catalyst and its overall effectiveness. In an acidic environment where the pH value is low, there is a rise in the production of hydroxide radicals (OH•) (Cheng et al., 2016). Additionally, the catalyst surface acquires a strong positive charge, which subsequently attracts negatively charged pollutants and water molecules. In the environments where the pH is elevated (alkaline conditions), there is an increase in the production of the negatively charged superoxide free radicals (O2•-), which are less efficient than hydroxide radicals (OH•) (Aljuboury et al., 2014). Furthermore, the catalyst surface becomes negatively charged and starts repelling water molecules, along with various pollutants that typically carry a negative charge. The performance of a catalyst can be influenced by its variety and the degree of its purity (Kazeminezhad, Sadollahkhani, 2016). Specifically, zinc oxide operates best in an environment where the pH is between 6 and 8 (Rajamanickam, Shanthi 2016). In EC, the efficiency of the process is significantly influenced by pH levels. This factor impacts both the adsorption and precipitation mechanisms within the process. Specifically, effective adsorption necessitates an alkaline

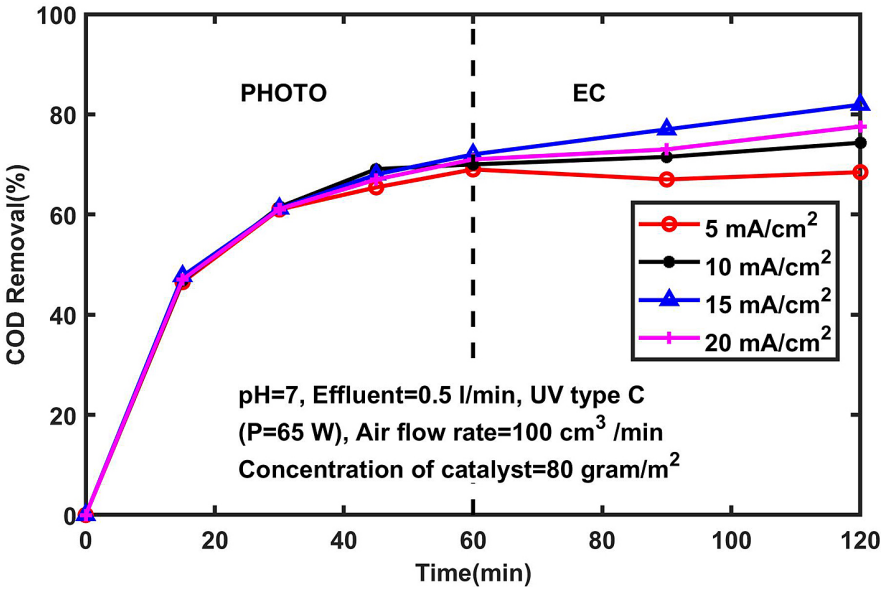

Figure 6. Effect of current density on combined sequential Photo-EC system-1

environment with a pH above 7. Conversely, optimum precipitation occurs under acidic conditions, requiring a low pH (İrdemez et al., 2021).

To identify the optimal pH level that yields the best outcomes for combined sequential Photo-EC system-1, four experiments were carried out. Figure 7 illustrates the initial removal efficiency of the photocatalysis process (first stage) at the beginning, midway through the first hour of the designated two-hour treatment period.

After the first hour, the removal percentages recorded were 67%, 72%, 75%, and 72% for initial pH values of 3, 5, 7, and 9, respectively. Figure 7 shows that the removal rates achieved at 120 minutes were 69%, 72%, 82%, and 77% for initial pH values of 3, 5, 7, and 9, respectively. The results presented above show that for the combined sequential Photo-EC system-1, the optimum removal efficiency was achieved at a pH of 7. Consequently, a pH of 7 was selected as best due to the highest removal efficiency. The findings show that the initial treatment stage (photocatalyst) is more effective than the subsequent stage (electrocoagulation). This efficiency is attributed to the fact that a pH level of 7 is highly conducive to the catalyst activity, facilitates the formation of a positive charge on the catalyst surface, and promotes the generation of hydroxide free radicals (Hansen et al., 2019). It is noteworthy that the pH remained stable and did not vary during the initial stage of treatment.

Some previous studies have shown that electrocoagulation needs an alkaline basic medium, whereas photocatalysis operates better in a slightly acidic medium. The conducted research found that a pH level near 7 yields the most effective results. A related study which used two distinct batch systems independently (EC and photocatalyst), indicating that a pH level of around 8.5 is optimal for treating wastewater in a simulated, rather than real wastewater (Garcia-Segura et al., 2017).

Effect of the total time on the performance of combined sequential systems

Figure 8 shows a comparison between the sequential EC-photo system-2 and the sequential photo-EC system-2 in which EC and photocatalytic processes were operated under the same conditions in section 3.2.1. except the total time was 60 min instead of 120 min. Figure 8 demonstrates that the efficiency with which sequential EC-photo system-2 removes contaminants is approximately 71%, closely matching that of the sequential EC-photo system -1. Similarly, the sequential photo -EC system-2 shows a removal efficiency of about 82% over a treatment duration of 60 minutes, which is similar to that of sequential photo -EC system-1 (120 min). In addition, there is a complete match in behavior during treatment between these systems. It was anticipated that the outcomes from sequential photo -EC system-1 and 2 would be accurate due to the optimum performance of both the photocatalytic and electrocoagulation processes individually, which is achieved within a duration not exceeding thirty

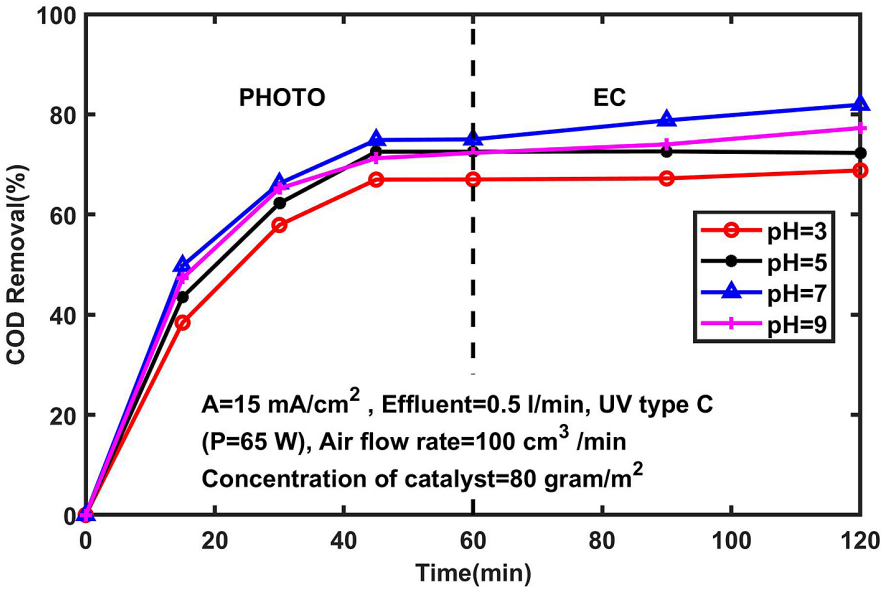

Figure 7. Effect pH on combined sequential Photo-EC system-1

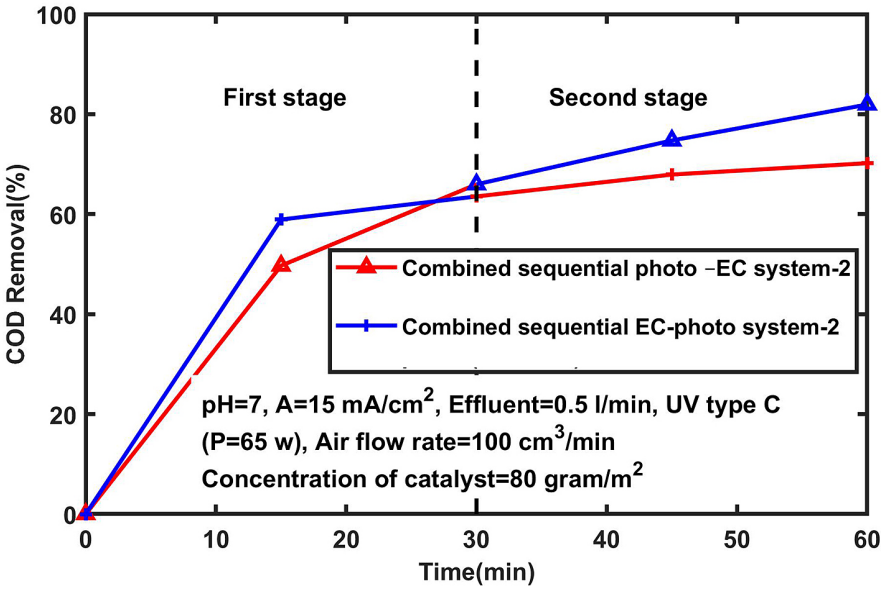

Figure 8. Combined sequential EC-photo system-2 + combined sequential photo –EC system-2

minutes. Following this duration, there is an observed rise in both turbidity and pH levels, accompanied by an increase in hydrogen bubbles, which adversely affects the performance of the integrated system.

For individual system, Akai discovered that the most effective results for the electrocoagulation technique are obtained at 39 minutes when utilizing aluminum as the anode and steel as the cathode. This process, which also incorporates titanium oxide, is optimal at a pH of approximately 6.5 and a current density of 22 mA/cm^2, enhancing the reduction of COD in wastewater from oil refineries. During this timeframe, the method successfully removed about 91% of COD. However, past this duration, the pH level escalated to over 10 and boosted the level of hydrogen bubbles, adversely impacting the efficiency of the treatment (Akkaya, 2022). In a similar experiment, the scientist conducted tests on the photocatalytic method to treat wastewater from refinery sources, utilizing optimal conditions included employing zinc oxide at a concentration of 3 g/L, maintaining a pH level of 10, and using UV light with a power of approximately 18 watts. Within a timeframe of 15–45 minutes, they achieved COD reduction rate of about 75%. Beyond this duration, the water turbidity increased, which diminished the penetration of solar light and consequently decreased (Mohammed, 2021)

For combined system, when examining other researchers who conducted a similar study but utilized a separate system for simulation, their processing time was about 180 minutes with a removal rate of 97% (Keramati, Ayati 2019). Another team of researchers evaluated a hybrid batch system that integrates an electrocoagulation method with a photocatalytic technique to purify wastewater used in lithography. The findings showed that the system was capable of eliminating 74% of the total organic demand (TOD). Specifically, the electrocoagulation method accounted for 65% of the reduction within 20 minutes, while the photocatalytic contributed to removing an additional 25% over a duration of 45 minutes. Consequently, the entire purification process took 65 minutes (Suárez-Escobar, Pataquiva-Mateus, López-Vasquez, 2016).

Simultaneous EC-photo system and simultaneous photo-EC system

Figure 9 shows a comparison between the simultaneous EC-photo system and simultaneous photo-EC system in which EC and photocatalytic processes were operated under the same conditions in section 3.1 except the time 60 min instead of 120 min with a total time of 120 min. Referring to Figure 9, it can be observed that after a 30 – minute period, simultaneous EC-photo system and simultaneous photo-EC system achieve elimination efficiencies of about 72% and 82%, respectively. These efficiency rates are maintained up 120 min. However, both systems cease functioning actually after the initial 30 minutes due to significant issues. Initially, simultaneous

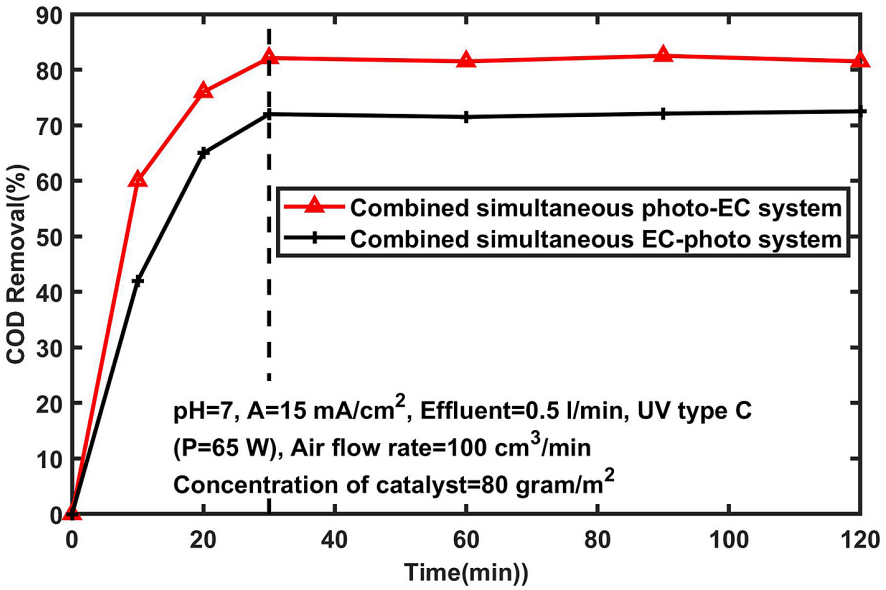

Figure 9. Combined simultaneous EC-photo system + combined simultaneous photo-EC system

EC-photo system encounters difficulties primarily due to foam formation, which eventually overwhelms the photoreactor. This issue is triggered by the emergence of hydrogen gas at the cathode electrode, interfering with the system's normal operations. Furthermore, the effectiveness of the photoreactor declines as slurry builds up within the system, impacting simultaneous EC-photo system more severely. Conversely, simultaneous photo-EC system experiences reduced efficiency predominantly because of the slurry ($Al(OH)_3$) accumulating in the flow resulting from electrocoagulation process, yet it manages to sustain a higher operational efficiency compared to simultaneous EC-photo system.

Asaithambi et al., 2024 analyzed the effectiveness of a hybrid simultaneous EC-photocatalyst batch system in processing industrial wastewater. The system operated under specific conditions: a pH level of 7, UV-C light at 40 watts, and a quantum current of 0.9 A. They achieved COD reduction rate of approximately 95% within a duration of 210 minutes (Asaithambi et al. 2024). Govindaraj et al., 2023 conducted a study on the elimination of bisphenol from water using a dual approach of electrocoagulation and photocatalysis (simultaneous system), employing titanium electrodes coated with metal oxides and utilizing zinc oxide as a photocatalyst. The findings showed that the electrocoagulation method accounted for a 59% reduction in bisphenol within 20 minutes, operating at a current of about 25 mA/cm^2 and a pH level around 8.9. Subsequently, the photocatalytic method achieved a complete removal rate of approximately 100%, over a duration of 90 minutes, with a zinc oxide concentration synthesized organically at roughly 100 mg/L and an irradiation power of about 15 watts.

Assessment of energy consumed and dissolution rate

The wastewater from the Diwaniyah refinery plant in Iraq underwent treatment using six different integrated systems. From these, three systems were identified as achieving the highest and equal removal rates. As depicted in Table 3, simultaneous photo –EC system stood out as the most efficient, requiring just 30 minutes to achieve its results and dissolution rate**.**

This affordable and efficient integrated system operates with minimal costs. Running this system for 30 minutes leads to very little sludge formation, which barely impacts the efficiency of the catalytic process. Consequently, the catalyst retains its surface efficiency and high performance throughout this time frame.

Kinetic studies in combined simultaneous photo –EC system

The study examined the kinetics of the system by analyzing four samples collected at intervals of 0, 10, 20, and 30 minutes over a half-hour period (valid duration). The correlation coefficients for both the pseudo-first order and

Table 3. Comparison between combined photo –EC systems

Integrated system model	Time (min)	Removal rate %	The energy consumed (KWh/Kg COD)	The dissolution rate (g)
Combined sequential photo – EC system-1	120	82	55.35	0.403
Combined sequential photo – EC system-2	60	82	28.44	0.281
Combined simultaneous photo – EC system	30	82	28.44	0.201

pseudo-second-order kinetic models were determined. The correlation values presented in Figures 10a and 10b show 81.27 for the pseudo-first-order equation and 98.86 for the pseudo-second-order equation, respectively.

Due to the significantly higher correlation coefficient of the pseudo-second-order kinetic model compared to the first, this model was subsequently adopted, as illustrated in the following Equation 15:

$$r = \frac{d[COD]}{dt} = -k[COD]^2 \quad (15)$$

where: the degradation rate, r (mg/L min), the reaction constant of degradation, k (mg/L.min), and the concentration of the organic substrate, *COD*, at any given time t (mg/L).

Once the Equation is integrated at $t = 0$, COD = COD_o (initial concentration), it transforms into the following form:

$$\frac{1}{[COD]} - \frac{1}{[COD]_o} = kt \quad (16)$$

To calculate the constant for a second-order reaction, the correlation between time and (1/[COD] - 1/$[COD]_o$) was depicted in the accompanying Figure 11a:

The kinetic data were adjusted using a pseudo-second order model, resulting in a constant k from equation 16 of 0.0001182 mg/L.min (Figure

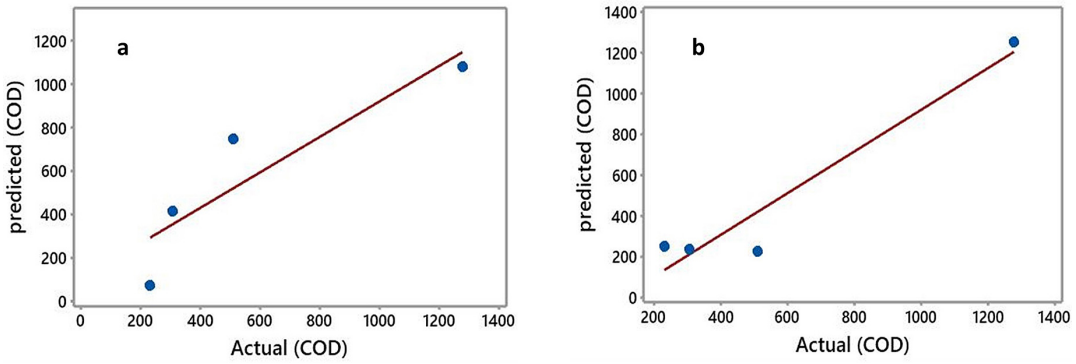

Figure 10. Data of actual versus date of predicted for COD elimination, (a) Linear (b) Full quadratic

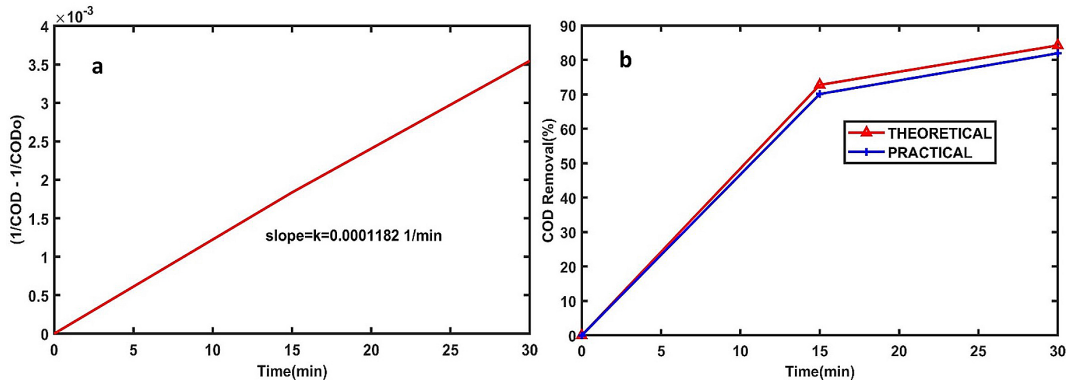

Figure 11. (a) Kinetic fit for combined simultaneous photo-EC system, (b) theoretical verses practical kinetic equation over time

11a), indicating that the process can be considered as adsorption. To evaluate the accuracy of the kinetic model, empirical data was compared with the results from the suggested kinetic mathematical model, as shown in Figure 11b. This comparison clearly supports the choice of the second-order kinetic model, as the model's predictions are in close agreement with the observed data. Previous works agreed with the findings of the present work, confirming that the reaction follows a pseudo second-order kinetic equation (Suárez-Escobar et al., 2016).

CONCLUSIONS

The purpose of this research was to eliminate COD by employing innovative, batch-recycle integrated systems for the first time. Through a series of experiments, it was determined that the most effective integrated system was simultaneous photo –EC system. This system achieved a removal rate of 82% with an operation time of 30 minutes, an energy consumption of approximately 28.44 kWh/kg COD and anode dissolution rate of approximately 0.2 gram. The best conditions were 15 mA/cm^2, pH of 7, flow rate of 0.5 L/min, ZnO concentration of 80 g/m^2, and 65 W. In addition to the brief operational duration of this system, there are several other benefits: creation of a very small amount of sludge that minimally impacts the photocatalytic process, the ease of separating this sludge at minimal cost, and the absence of flooding caused by hydrogen gas release in the photocatalytic reactor.

Results showed that if EC was applied initially, an increase in pH levels occurred. This increase adversely affects the efficiency of the subsequent photocatalytic process in the sequence of treatment. Consequently, the effectiveness of the photocatalytic process is reduced due to this pH change (EC-photo sequential system-1,2). On the other hand, starting with the photocatalytic process keeps the pH levels stable, which does not interfere with the electrocoagulation process applied afterwards (photo -EC sequential system-1,2). As a result, implementing the photocatalytic process first results in a more successful treatment.

Acknowledgements

The authors express their gratitude for the invaluable insights, assistance, and technical assistance they received from staff of the Department of Chemical Engineering, College of Engineering, University of Baghdad.

REFERENCES

1. Abdulredha, M.M., Siti Aslina, H. and Luqman, C.A. 2020. Overview on petroleum emulsions, formation, influence and demulsification treatment techniques. Arabian Journal of Chemistry. 13(1), 3403–3428. DOI 10.1016/J.ARABJC.2018.11.014.
2. Akkaya, G.K. 2022. Treatment of petroleum wastewater by electrocoagulation using scrap perforated (Fe-anode) and plate (Al and Fe-cathode) metals: Optimization of operating parameters by RSM. Chemical Engineering Research and Design. 187, 261–275. DOI 10.1016/J.CHERD.2022.08.048.
3. Al Mayyahi, A. and Al-Asadi, Hamid A.A. 2018. Advanced oxidation processes (AOPs) for wastewater treatment and reuse: A brief review. Asian J. Appl. Sci. Technol. 2, 18–30.
4. Aljuboury, A., Palaniandy P., Bin H., Aziz A. 2014. A review on the Fenton process for wastewater treatment. [online]. 2(3), p. undefined-undefined. Retrieved from: https://www.mendeley.com/catalogue/3954d040-b0e8-38e7-92f5-f707950a7383/ [accessed 19 July 2024].
5. Almomani, Fares A., Shawaqfah M., Bhosale R.R., Kumar A. 2016. Removal of emerging pharmaceuticals from wastewater by ozone-based advanced oxidation processes. Environmental Progress and Sustainable Energy. 35(4), 982–995. DOI 10.1002/EP.12306.
6. Almomani, F., Bhosale, R., Kumar, A., Khraisheh, M. 2018. Potential use of solar photocatalytic oxidation in removing emerging pharmaceuticals from wastewater: A pilot plant study. Solar Energy. 172, 128–140. DOI 10.1016/J.SOLENER.2018.07.041.
7. Al-Rubaiey, N.A., Albrazanjy, M.G. and Kadhim, W.A. 2022. Combined electrocoagulation and photocatalytic for oily wastewater treatment using TiO2 nano-catalysts. Egyptian Journal of Chemistry. 65(7), 55–64. DOI 10.21608/EJCHEM.2021.89321.4286.
8. Asaithambi, P., Desta, W.M., Yesuf, M.B., Hussen, M., Asmelash, Z., Beyene, D., Periyasamy, S., Alemayehu, E. 2024. Photo-alternating current-electrocoagulation technique: Studies on operating parameters for treatment of industrial wastewater. Scientific African. 24, e02193.
9. Ben Hariz, I., Halleb, A., Adhoum, N., Monser, L. 2013. Treatment of petroleum refinery sulfidic spent caustic wastes by electrocoagulation. Separation and Purification Technology. 107, 150–157. DOI 10.1016/J.SEPPUR.2013.01.051.
10. Cao, J., Cao J., Yang, J., Yue, K., Wang, Z. 2020. Preparation of modified citrus pectin (MCP) using

an advanced oxidation process with hydroxyl radicals generated by UV-H2O2. Food Hydrocolloids. 102. DOI 10.1016/J.FOODHYD.2019.105587.

11. Cheng, M., Zeng, G., Huang, D., Lai, C., Xu, P., Zhang, C, Liu, Y. 2016. Hydroxyl radicals based advanced oxidation processes (AOPs) for remediation of soils contaminated with organic compounds: A review. Chemical Engineering Journal. 284, 582–598. DOI 10.1016/J.CEJ.2015.09.001.
12. Delnavaz, M., Ayati, B., Ganjidoust, H., Sanjabi S. 2011. Optimization of photo-catalytic process by TiO_2 nano powder immobilized on concrete surface for treatment of phenolic wastewater. Environmental Engineering and Management Journal. 10, 10. DOI 10.30638/eemj.2011.206.
13. Demirbas, E. And Kobya, M. 2017. Operating cost and treatment of metalworking fluid wastewater by chemical coagulation and electrocoagulation processes. Process Safety and Environmental Protection. 105. DOI 10.1016/j.psep.2016.10.013.
14. Elmobarak, W.F., Hameed, B.H., Almomani, F, Abdullah, A.Z. 2021. A Review on the Treatment of Petroleum Refinery Wastewater Using Advanced Oxidation Processes. Catalysts. 11(7), undefined-undefined. DOI 10.3390/CATAL11070782.
15. El-Naas, M.H., Alhaija, M.A. and Al-Zuhair, S. 2014. Evaluation of a three-step process for the treatment of petroleum refinery wastewater. Journal of Environmental Chemical Engineering. 2(1), 56–62. DOI 10.1016/J.JECE.2013.11.024.
16. Fahem, A.S. and Abbar, A.H. 2020. Treatment of petroleum refinery wastewater by electro-Fenton process using porous graphite electrodes. Egyptian Journal of Chemistry. 63(12), 4805–4819. DOI 10.21608/EJCHEM.2020.28148.2592.
17. García-García, A., Martínez-Miranda, V., Martínez-Cienfuegos, I.G., Almazán-Sánchez P.T., Castañeda-Juárez M., Linares-Hernández, I. 2015. Industrial wastewater treatment by electrocoagulation-electrooxidation processes powered by solar cells. Fuel. 149, 46–54. DOI 10.1016/J.FUEL.2014.09.080.
18. Garcia-Segura, S., Eiband, M.M.S.G., de Meloet J.V. 2017. Electrocoagulation and advanced electrocoagulation processes: A general review about the fundamentals, emerging applications and its association with other technologies. Journal of Electroanalytical Chemistry. 801, 267–299. DOI 10.1016/J.JELECHEM.2017.07.047.
19. Ghanbari, F., Khatebasreh, M., Mahdavianpour M., Lin, K.-Y.A. 2020. Oxidative removal of benzotriazole using peroxymonosulfate/ozone/ultrasound: Synergy, optimization, degradation intermediates and utilizing for real wastewater. Chemosphere. 244. DOI 10.1016/J.CHEMOSPHERE.2019.125326.
20. Govindaraj, M., Babu, S., Rathinam, R., Vasini, V. and Vijayakumar K. 2023. Integrated electrocoagulation–photo electrocatalytic oxidation for effective treatments of aqueous solution bisphenol-A using green-synthesized ZnO nanoparticles. Chemical Papers. 77(1), 169–183.
21. Hansen, H.K., Peña, S.F., Gutiérrez, C., Lazo, A., Lazo P., Ottosen L.M. 2019. Selenium removal from petroleum refinery wastewater using an electrocoagulation technique. Journal of Hazardous Materials. 364, 78–81.
22. İrdemez, Ş., Bingül Z., Kul, S., Torun, F.E., Demircioğlu - El-Cezeri, N. 2021. The effect of pH on removal of phosphate from water using aluminum electrodes by electrocoagulation method. El-Cezeri Journal of Science and Engineering. 8(3), 1472–1479. DOI 10.31202/ECJSE.948309.
23. Jafarinejad, S. and Jiang, S.C. 2019. Current technologies and future directions for treating petroleum refineries and petrochemical plants (PRPP) wastewaters. Journal of Environmental Chemical Engineering. 7(5). DOI 10.1016/J.JECE.2019.103326.
24. Jiménez, S., Andreozzi M., Micó M.M., Álvarez M.G., Contreras S. 2019. Produced water treatment by advanced oxidation processes. Science of the Total Environment. 666, 12–21. DOI 10.1016/J.SCITOTENV.2019.02.128/PRODUCED_WATER_TREATMENT_BY_ADVANCED_OXIDATION_PROCESSES.PDF.
25. Kazeminezhad, I. and Sadollahkhani, A. 2016. Influence of pH on the photocatalytic activity of ZnO nanoparticles. Journal of Materials Science: Materials in Electronics. 27, 5. DOI 10.1007/s10854-016-4284-0.
26. Keramati, M. and Ayati, B. 2019. Petroleum wastewater treatment using a combination of electrocoagulation and photocatalytic process with immobilized ZnO nanoparticles on concrete surface. Process Safety and Environmental Protection. 126, 356–365. DOI 10.1016/J.PSEP.2019.04.019.
27. Li, D., Sun, T., Wang, L., Wang N. 2018. Enhanced electro-catalytic generation of hydrogen peroxide and hydroxyl radical for degradation of phenol wastewater using MnO2/Nano-G|Foam-Ni/Pd composite cathode. Electrochimica Acta. 282, 416–426. DOI 10.1016/J.ELECTACTA.2018.06.075.
28. Mohammed, S.A. 2021. Treatment of organic compounds resulting from oil refineries under solar light and reuse it for industrial purpose. Muthanna Journal of Engineering and Technology. DOI 10.52113/3/eng/mjet/2021-09-01/20-24.
29. Mohd Adnan, M.A., Bao, L.P. and Muhd, J.N. 2020. Mitigation of pollutants by chitosan/metallic oxide photocatalyst: A review. Journal of Cleaner Production. 261. DOI 10.1016/J.JCLEPRO.2020.121190.
30. Qu, R., Li, C., Liu, J., Xiao, R., Pan, X., Zenget, X. 2018. Hydroxyl radical based photocatalytic degradation of halogenated organic contaminants

and paraffin on silica gel. Environmental Science and Technology. 52(13), 7220–7229. DOI 10.1021/ACS.EST.8B00499.

31. Rajamanickam, D. and Shanthi, M. 2016. Photocatalytic degradation of an organic pollutant by zinc oxide – solar process. Arabian Journal of Chemistry. 9, 1858–1868. DOI 10.1016/J.ARABJC.2012.05.006.
32. Raza, W., Lee, J., Raza, N., Luo, Y., Kim, K.H. 2019. Removal of phenolic compounds from industrial wastewater based on membrane-based technologies. Journal of Industrial and Engineering Chemistry. 71, 1–18. DOI 10.1016/J.JIEC.2018.11.024.
33. Rostam, A.B. and Taghizadeh, M. 2020. Advanced oxidation processes integrated by membrane reactors and bioreactors for various wastewater treatments: A critical review. Journal of Environmental Chemical Engineering. 8(6). DOI 10.1016/J.JECE.2020.104566.
34. Sathasivam, M., Shanmugapriya, S., Venkatraman, Y., Ak, P. 2019. Industrial waste water treatment using advanced oxidation process–A review. Int. J. Eng. Adv. Technol. 8(3), 485–488.
35. Sonu, Dutta V., Sharma S., Raizada P., Hosseini-Bandegharaei A., Gupta V.K., Singh P. 2019. Review on augmentation in photocatalytic activity of CoFe2O4 via heterojunction formation for photocatalysis of organic pollutants in water. Journal of Saudi Chemical Society. 23(8), 1119–1136. DOI 10.1016/J.JSCS.2019.07.003.
36. Suárez-Escobar, A., Pataquiva-Mateus, A. and López-Vasquez, A. 2016. Electrocoagulation - Photocatalytic process for the treatment of lithographic wastewater. Optimization using response surface methodology (RSM) and kinetic study. Catalysis Today. 266, 120–125. DOI 10.1016/J.CATTOD.2015.09.016.
37. Varjani, S.J. 2017. Bioresource Technology Microbial degradation of petroleum hydrocarbons. [online]. 223, 277–286. Retrieved from : https://www.mendeley.com/catalogue/e03b3294-433b-3d10-b57b-30b05fa3578d/ [accessed 13 July 2024].
38. Varjani, S., Kumar, G. And Rene, E.R. 2019. Developments in biochar application for pesticide remediation: Current knowledge and future research directions. Journal of Environmental Management. 232, 505–513. DOI 10.1016/J.JENVMAN.2018.11.043.
39. Wan, Q. 2023. Recent advances in the electrochemical generation of 1,3-dicarbonyl radicals from C-H bonds. Organic Chemistry Frontiers. 10(11), 2830–2848. DOI 10.1039/D3QO00408B.
40. Yang, Y. and Hoffmann, M.R. 2016. Synthesis and Stabilization of Blue-Black TiO2 Nanotube Arrays for Electrochemical Oxidant Generation and Wastewater Treatment. Environmental Science and Technology, 50(21), 11888–11894. DOI 10.1021/ACS.EST.6B03540.
41. Yavuz, Y. and Ögütveren, B. 2018. Treatment of industrial estate wastewater by the application of electrocoagulation process using iron electrodes. Journal of Environmental Management. 207, 151–158. DOI 10.1016/J.JENVMAN.2017.11.034.
42. Zhang, X., He, W., Ren, L., Stager, J., Evans, P.J. 2015. COD removal characteristics in air-cathode microbial fuel cells. Bioresource Technology. 176, 23–31. DOI 10.1016/J.BIORTECH.2014.11.001.